Spectral analysis of time-limited pulsed Gaussian wave fields

Amr M. Shaarawi, Sherif M. Sedky, and Fawzia M. M. Taiel

Department of Engineering Physics and Mathematics, Faculty of Engineering, Cairo University, Giza, Egypt

Richard W. Ziolkowski

Electromagnetics Laboratory, Department of Electrical and Computer Engineering, University of Arizona, Tuscon, Arizona 85721

Ioannis M. Besieris

Bradley Department of Electrical Engineering, Virginia Polytechnic Institute State University, Blacksburg, Virginia 24061

Received June 29, 1995; accepted December 21, 1995; revised manuscript received January 18, 1996

We compare the depletion of the spectral components of pulsed wave fields as they propagate away from their sources. The spectral performance of a narrow localized Gaussian pulse launched from a dynamic aperture is compared with that of the traditional Gaussian-waisted, quasi-monochromatic, and broadband signals generated by flat apertures. The effect of using a derivative receiver to slow down the decay rate of the measured localized wave fields is expounded upon by using the same spectral analysis. © 1996 Optical Society of America.

1. INTRODUCTION

Brittingham's[1] proposal of the nondispersive focus wave mode (FWM) solution to Maxwell's equations resulted in an ample investigation of ultrawide bandwidth signals exhibiting extended ranges of localization. The original FWM field is characterized by having an infinite total energy content.[2] However, a class of finite-energy field solutions has been deduced by using superpositions of the source-free FWM.[3] Such a class of pulsed wave fields has become known as localized waves[4–10] (LW). The generation and transmission of such fields have been studied extensively. The LW pulses are characterized by a strong coupling between their spatial and temporal spectral components.[11,12] Such a connection exists over all of their ultrawide spatial–temporal bandwidths. This property is reminiscent of the original FWM field. Furthermore, it has been demonstrated that the coupling allows the generated pulses to propagate with very little dispersion over extended ranges.[8,11,12]

In a recent study[11] it was shown that a very good approximation to the scalar FWM pulse can be launched from a dynamic aperture excited for an infinitely long period of time. Since such an infinite illumination is not practical, one may resort to time limiting the initial FWM excitation of the aperture.[12] In a study of the finite-illumination scheme, it was shown that the use of dynamic apertures provides an efficient method to generate pulses of narrow Gaussian waists from extended sources of much larger dimensions. Similarly to all other LW solutions, the approximation to the FWM pulse generated from a finite-time dynamic aperture exhibits a close coupling between its spatial and temporal spectral components. In fact such a spectral correlation allows the generated LW pulse to outperform Gaussian beams characterized by single carrier frequencies. In such a comparison[12] we assumed that the continuous wave (CW) Gaussian beam is generated from a static aperture of the same extension as the maximum radius of the dynamic source. The focused waist of the CW beam and of the LW pulse are taken to be equal. Furthermore, the carrier frequency of the CW is chosen to be equal to the highest temporal frequency component of the illumination wave field of the dynamic aperture. One can then show (see Ref. 12) that the half-amplitude range of the LW pulse generated from a dynamic aperture is several orders of magnitude larger than that of the Gaussian beam generated from a static aperture.

The study of the effects of time limiting the excitation of a dynamic FWM aperture on the depletion of the spectral components of the generated wave field shows exactly how the centroid of the LW pulse holds out for the extended range mentioned above and why, beyond such a point, it starts to spread out. Various time-limiting schemes as well as spatial spectral distributions have been investigated. In this study we demonstrate that the spectral depletion of the frequency components of LW pulses generated from dynamic apertures is completely different in nature from that of other transient pulsed wave fields having the same waist and longitudinal time duration. We compare the spectral depletion of the Gaussian-waisted LW pulse generated by a FWM dynamic source with that of a quasi-monochromatic time-limited pulse having the same Gaussian waist but

0740-3232/96/0901827-10$10.00

launched from a static aperture. The switching time intervals of the excitations of those two pulsed fields are taken to be equal. Furthermore, to clarify some aspects of the comparison, we include a third case of a transient beam having a broad spectral width. For the latter case, the longitudinal dimension of such a broadband pulse is chosen to be of the same order of magnitude as the length of the central portion of the FWM pulse. Finally, we demonstrate the effect of the measurement of a FWM pulse with a derivative detector.[13]

2. EXCITATION OF TIME-LIMITED WAVE FIELDS

Consider the following representation of an azimuthally symmetric illumination of a flat aperture located at $z = 0$:

$$\Psi_i(\rho, t) = \mathrm{Re}\{\hat{\Psi}_i(\rho, t)\}, \tag{2.1a}$$

where

$$\hat{\Psi}_i(\rho, t) = \left(\frac{1}{2\pi}\int_0^\infty \mathrm{d}\chi\chi J_0(\chi\rho)\int_0^\infty \mathrm{d}\omega\,\phi(\chi, \omega) \times \exp\{-i[\sqrt{(\omega/c)^2 - \chi^2}]z\}\exp(i\omega t)\right)_{z=0}. \tag{2.1b}$$

Here ω is the temporal angular frequency and χ is the transverse spatial spectral variable. For a time-limited wave field characterized by an initial waist w and a finite period of excitation equal to $4T$, we define the Fourier spectrum as follows:

$$\phi(\chi, \omega) = \frac{T}{\sqrt{\pi}}\{\exp -T^2[\omega - \omega_0(\chi)]^2\}\exp(-\chi^2 w^2). \tag{2.2}$$

One should note that $\omega_0(\chi)$ depends on χ. Such a connection allows the spatial–temporal spectra to be coupled together. The study of the effect of the spatial–temporal coupling on the depletion of the spectral components of the LW pulses with distance is the main aim of this work. Before we can proceed in that direction, we need to recapitulate some aspects of the thoroughly investigated case of a time-limited pulse that has an effective duration limited to the interval $[-4T, 4T]$ and whose spatial and temporal spectral components are independent of each other. This independence can be achieved if we choose $\omega_0(\chi) = \omega_c$, where ω_c is a carrier frequency of a constant value independent of χ. Nevertheless, there are two limits for such a choice. Specifically, for $\omega_c \gg 1/T$ the generating aperture is excited for a time interval that is much larger than the oscillation period of any significant spectral components contributing to the illumination wave field. Consequently, the Gaussian ω window introduced in Eq. (2.2) has a narrow spectral width in comparison with the carrier frequency ω_c. The field representation defined in Eq. (2.1) thus depicts a quasi-monochromatic signal. In the other limit, we choose $\omega_c \sim O(1/T)$. The Gaussian in Eq. (2.2) hence acquires a spectral width comparable to that of the carrier frequency. Such a limit corresponds to having a broad-band signal. In both limits we substitute $\omega_0(\chi) = \omega_c$ into Eqs. (2.1) and (2.2) and carry out the integrations over χ and ω to obtain

$$\hat{\Psi}_i(\rho, t) = \frac{1}{4\pi w^2}\exp(-\rho^2/4w^2)\exp(-t^2/4T^2) \times \exp(+i\omega_c t). \tag{2.3}$$

The above expression for the illumination wave field confirms our previous assertions that w, $4T$, and ω_c represent the waist, the duration of the excitation, and the carrier frequency, respectively. Hence Eq. (2.3) represents a time-limited pulse characterized by a waist equal to w and a temporal duration $4T$. We assume that such a field is launched from a flat aperture situated at $z=0$. The effective radius of the aperture is always equal to w even if the aperture has a larger physical dimension. This is the case because the $\exp(-\rho^2/4w^2)$ term fixes the radius of the aperture for the whole duration of the source illumination. Note also that in the extreme limit $T \to \infty$, the Gaussian function in Eq. (2.2) becomes a Dirac δ function, and the field in (2.2) reduces to that of a monochromatic Gaussian beam.

Now we consider the case in which the temporal and the spatial spectral components are coupled together:

$$\omega_0(\chi) = (\chi^2/4\beta + \beta)c, \tag{2.4}$$

where the specific choice of the parameter β and the shape of $\omega_0(\chi)$ yield a FWM excitation (see Refs. 11 and 12). The relationship given in Eq. (2.4) indicates that the center of the Gaussian ω window in Eq. (2.2) varies as a function of the transverse spectral variable χ. When the integration in Eq. (2.1) is performed over χ, the ω window sweeps the whole bandwidth of the χ spectrum that is specified by the spatial Gaussian $\exp(-\chi^2 w^2)$. Furthermore, the time interval T determines the width of the temporal ω window, which decreases as T is increased. Substituting Eq. (2.4) into Eqs. (2.1) and (2.2) and integrating over χ and ω, we obtain

$$\hat{\Psi}_i = \frac{\beta}{\pi(a_1 - ict)}\exp[-\beta\rho^2/(a_1 - ict)]\exp(i\beta ct) \times \exp(-t^2/4T^2), \tag{2.5}$$

where, for convenience, we have substituted $w = \sqrt{a_1/4\beta}$. This is the FWM illumination wave field used in previous studies[8,11,12] as an excitation of a dynamic Gaussian aperture capable of generating a good approximation to the FWM pulse in the near-to-far-field region. Notice that the initial illumination has a minimum radius $R_{\min} = 2w$, and for $ct \gg a_1$ the radius varies with time such that it is effectively equal to $ct/\sqrt{\beta a_1}$. The interval of excitation $[-4T, 4T]$ thus determines the maximum size of the aperture. In the above-mentioned investigations, it has also been stressed that the condition $\beta a_1 \ll 1$ is necessary to ensure that a causal FWM pulse is efficiently generated by a dynamic aperture.[11] Furthermore, in a comparison between the FWM pulse and a strictly monochromatic Gaussian beam with the same waist, it has been shown that the FWM pulse holds out to much larger distances.[12] In this comparison the monochromatic frequency was chosen to be equal to the

maximum-frequency component of the temporal bandwidth $\omega_{\max} = 4/a_1$ of the FWM wave field. In this paper we extend the comparison to time-limited pulses of the same waist, using the excitation field given in Eq. (2.3). We demonstrate how the decay of the amplitude of such pulses as they travel away from the aperture is related to the depletion of their frequency content. There are fundamental differences between the removal of the spectral components with distance of the LW pulse generated by the initial wave field [Eq. (2.5)] and the quasi-monochromatic or broadband signals excited by Eq. (2.3).

The excitation wave fields of the three cases mentioned above generate pulses that have different propagation characteristics. Huygen's construction[14] together with the initial illumination given in Eq. (2.1) may be used[11,12] determine the amplitude of the pulsed wave field as it propagates away from the aperture into the $z > 0$ half-space. Furthermore, we can deduce from Eq. (2.1) the normal derivative on the aperture substituted into the Huygen's formula by differentiating with respect to z before we set $z = 0$. It has been previously shown (see Refs. 11 and 12) that the field radiated from an aperture located at $z = 0$ and illuminated by Ψ_i given in Eq. (2.1) becomes equal to

$$\Psi(\rho, z, t) = \mathrm{Re}[\hat{\Psi}(\rho, z, t)], \tag{2.6a}$$

where

$$\hat{\Psi}(\rho, z, t) = \frac{1}{2\pi}\int_0^\infty \mathrm{d}\chi\chi J_0(\chi\rho)\int_0^\infty \mathrm{d}\omega\,\phi(\chi,\omega)\exp(i\omega t) \times \exp\{-i[\sqrt{(\omega/c)^2 - \chi^2}]z\}. \tag{2.6b}$$

Here we are interested only in the propagating-field components. The evanescent modes[11] are cut off by the condition $(\omega/c) > \chi$. The FWM field propagating in the $z > 0$ half-space can hence be obtained by substituting Eqs. (2.2) and (2.4) into Eq. (2.6):

$$\Psi(\rho, z, t) = \frac{T}{2\pi^{3/2}}\int_0^\infty \mathrm{d}\chi\chi J_0(\chi\rho) \times \int_0^\infty \mathrm{d}\omega\,\exp\{-T^2[\omega - \omega_0(\chi)]^2\} \times \exp(-\chi^2 w^2)\cos\{[\sqrt{(\omega/c)^2 - \chi^2}]z - \omega t\}. \tag{2.7}$$

Fig. 1(a) displays the decay pattern of the center of the FWM pulse at distances $z = ct$ that are integer multiples of π/β. In this figure we have used the parameter values $a_1 = 0.00001$ m, $cT = 6.25$ mm, and $\beta = 1.25\ \mathrm{m}^{-1}$. The radius of the generated pulse is equal to $R_{\min} = 2w = 2.828$ mm and $\omega_{\max} = 4c/a_1 = 1.2 \times 10^{14}$ rad/s. At this point it is instructive to compare the decay pattern of the FWM pulse with that of other traditional signals in order to show that the FWM pulse holdsout better for farther distances. The field associated with the time-limited signal [Eq. (2.3)] is obtained by substituting Eq. (2.2), with $\omega_0(\chi) = \omega_c$, into Eq. (2.6); specifically,

$$\Psi(\rho, z, t) = \frac{T}{2\pi^{3/2}}\int_0^\infty \mathrm{d}\chi\chi J_0(\chi\rho) \times \int_0^\infty \mathrm{d}\omega\,\exp[-T^2(\omega - \omega_c)^2] \times \exp(-\chi^2 w^2)\cos[\sqrt{(\omega/c)^2 - \chi^2}z - \omega t]. \tag{2.8}$$

For $\omega_c \gg 1/T$, we have a quasi-monochromatic signal, whereas the other limit with $\omega_c \sim O(1/T)$ produces a

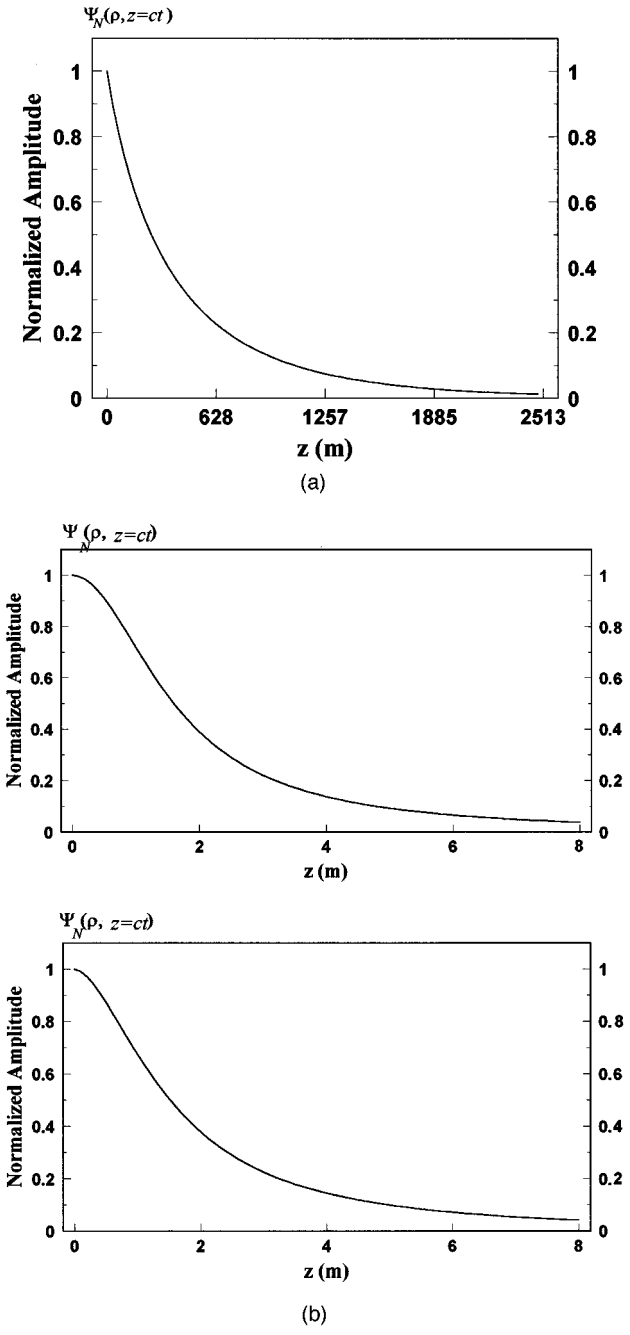

Fig. 1. Decay of the centroid of time-limited pulses: (a) FWM pulse, (b) quasi-monochromatic (top) and broadband (bottom) signals.

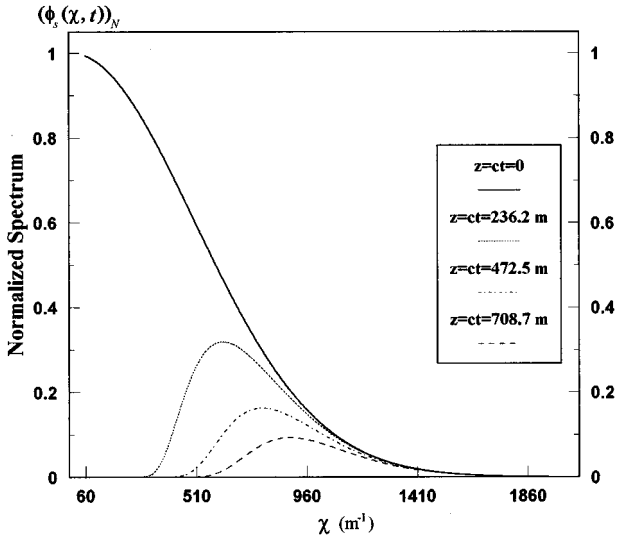

Fig. 2. The depletion of the FWM spatial spectrum with distance.

broadband signal. The amplitude given in Eq. (2.8) is plotted in Fig. 1(b) at $z = ct$, for $\omega_c = 4c/a_1 = 1.2 \times 10^{14}$ rad/s, $w = \sqrt{a_1/4\beta} = 1.414$ mm and, $cT = 6.25$ mm. These values correspond to the quasi-monochromatic case. Note that the carrier frequency is equal to the $1/e^4$ point of the temporal spectrum of the FWM pulse. For the broadband excitation we change cT to a value of 5×10^{-3} mm. Hence these two signals have the same waist as that of the FWM pulse. The quasi-monochromatic signal, however, has a longitudinal extension equal to that of the total radiated FWM field. On the other hand, the broadband signal has a length that equals a_1; this parameter characterizes the longitudinal extension of the highly focused central portion of the FWM pulse. It is clear from Fig. 1(b) that the decay patterns of the quasi-monochromatic and the broadband signals are almost identical. It is obvious from Fig. 1(a) that the amplitude of the FWM pulse drops to half its value at $z = 245$ m, while the half-amplitude distance corresponding to the two other time-limited signals is 1.6 m. The FWM dynamic aperture thus is capable of sending focused LW pulses with very little dispersion over distances several orders of magnitude larger than the distances traveled by other time-limited pulses with the same waist.

A flat expanding aperture, hence, is an efficient contraption that may be used to send pulses of narrow waists to far distances, at the expense of the source acquiring larger sizes. For such a dynamic source, the generated pulse makes full use of the size of its source. In contrast, a quasi-monochromatic excitation of a similar narrow Gaussian from a static aperture that is equal in size to the FWM maximum radius makes no use whatever of the extra extent of its source; it utilizes only the portion of the aperture with $r < R_{\min}=2w$. A comparison with the performance of pulses that have larger Gaussian waists generated from larger static apertures is thus futile, because we would be comparing two wave fields of different focused radii.

Before proceeding to the next section, we would like to comment on the fact that the FWM wave field has the same longitudinal extension cT as the quasi-monochromatic pulse. Nevertheless, the generated FWM pulse is carrier free, and its total bandwidth is not determined solely by the pulse interval T. Instead, its overall temporal bandwidth is a cumulative product of the juxtaposition of the individual ω windows as they sweep the whole χ spectrum. The resulting temporal bandwidth $\Delta\omega \cong O(c/a_1)$ is much larger than the spectral width of the Gaussian window associated with the quasi-monochromatic pulse, namely, $\delta(\omega) \sim O(1/T)$. For this reason the excitation of the FWM field is usually referred to as having an ultrawide bandwidth, even though the whole FWM wave field is not very short. Nevertheless, the focused central portion of the FWM pulse is ultrashort, and its length is of the order of magnitude of a_1. One should note also that a_1 is inversely proportional to the total temporal frequency bandwidth of the FWM pulse.[12]

3. DEPLETION OF THE SPATIAL SPECTRA OF THE TIME-LIMITED WAVE FIELDS

To understand the decay of the amplitude of the aforementioned time-limited signals as they propagate away from their sources, one should look at the associated spatial spectra and their depletion with distance. We define the spatial spectrum at any distance z from the aperture as

$$\phi_s(\chi, z, t) = \frac{1}{2\pi}\int_0^\infty d\omega\,\phi(\chi,\omega)\cos\{[\sqrt{(\omega/c)^2 - \chi^2}]z - \omega t\}. \tag{3.1}$$

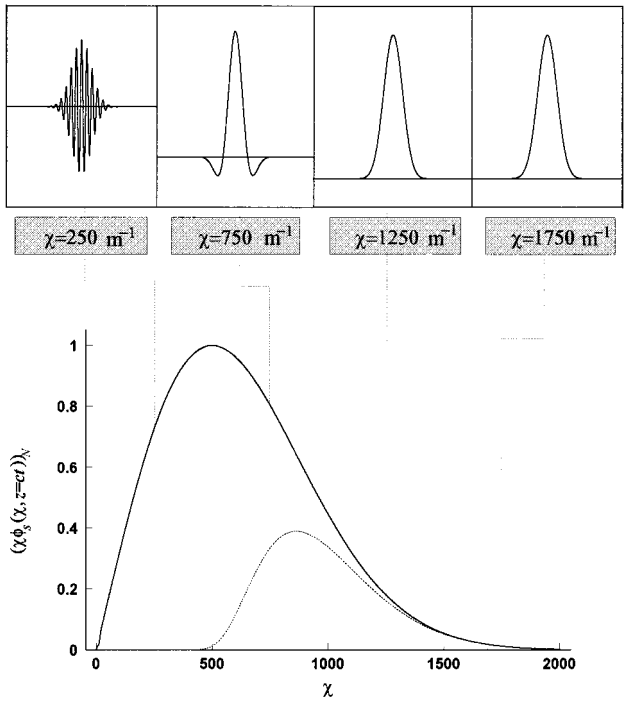

Fig. 3. Oscillations that affect different sections of the FWM spatial spectrum at $z = ct = 525.27$ m. Solid curve, $\chi\phi_s(\chi, z = ct = 0)$; dotted curve, $\chi\phi_s(\chi, z = ct = 525.27$ m).

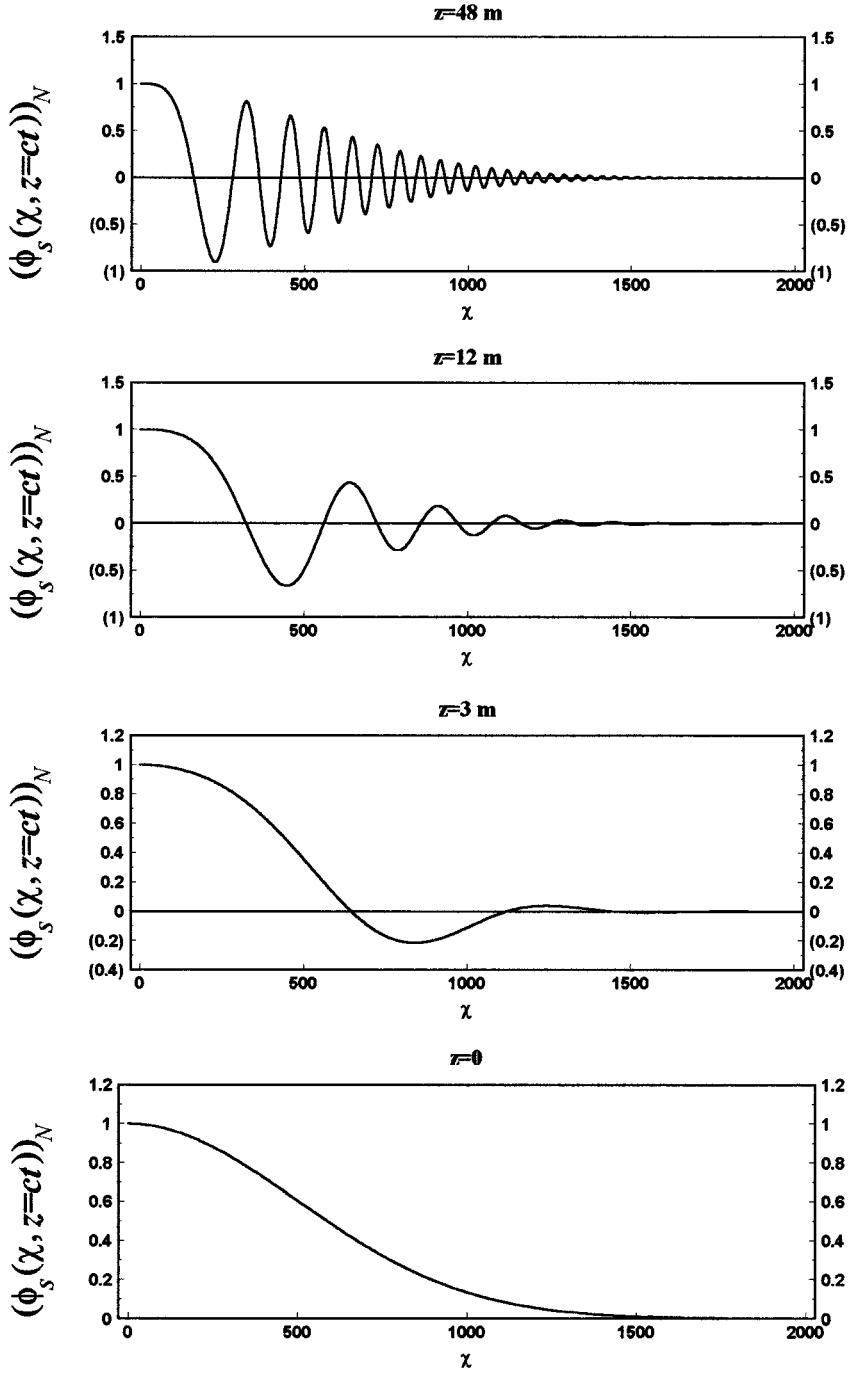

Fig. 4. Depletion of the spatial spectrum of the quasi-monochromatic CW signal with distance.

With Eqs. (3.1) and (2.6) the field propagating in the $z > 0$ half-space can be rewritten as

$$\Psi(\rho, z, t) = \int_0^\infty \phi_s(\chi,z,t)\chi J_0(\chi\rho)\mathrm{d}\chi. \tag{3.2}$$

The spatial spectrum of the FWM pulse is obtained by substituting Eqs. (2.2) and (2.4) into Eq. (3.1), which yields

$$\phi_s(\chi, z, t) = \frac{T \exp(-\chi^2 w^2)}{2\pi^{3/2}} \int_0^\infty \mathrm{d}\omega \exp\{-T^2[\omega - \omega_0(\chi)]^2\} \times \cos\{[\sqrt{(\omega/c)^2 - \chi^2}]z - \omega t\}. \tag{3.3}$$

The integrand in Eq. (3.3) embodies a Gaussian ω window centered at $\omega_0(\chi)$ and effectively extending between $\omega_0(\chi) - 4/T$ and $\omega_0(\chi) + 4/T$. For the FWM excitation this ω-window acts as an envelope of the cosine term in

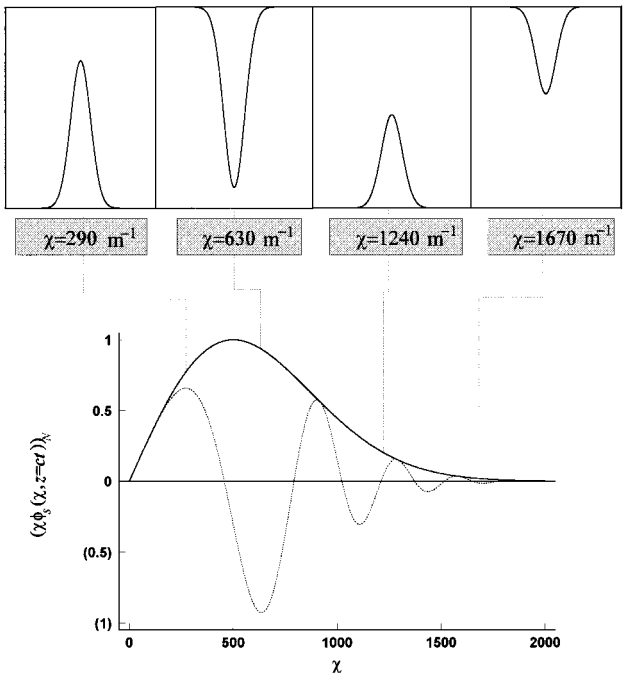

Fig. 5. Oscillations that affect different sections of the spatial spectrum of the quasi-monochromatic CW signal at $z = ct = 6$ m. Solid curve, $\chi\phi_s(\chi, z = ct = 0)$; dotted curve, $\chi\phi_s(\chi, z = ct = 6\ \text{m})$.

the integrand. The envelope sweeps the whole χ spectrum when the integration over χ in Eq. (3.2) is performed. The oscillations of the cosine term depend on both χ and z. For a given value of z the number of oscillations incorporated within a specific window is inversely proportional to χ. Figures 2 and 3 clarify this issue. The spatial spectrum given in Eq. (3.3) is plotted in Fig. 2 at various values of $z = ct$. It is clear from the figure that the low χ components are depleted faster than the higher ones. As the pulse travels to farther distances, the depletion of the low-frequency spatial components is increased. To understand the nature of such depletion of the spatial spectrum, one can refer to Fig. 3. In this figure we display the changes in $[\chi\phi_s(\chi, z = ct)]$ as the pulse propagates away from the aperture. Note that the area under the $\chi\phi_s(\chi, z = ct)$ curve [see Eq. (3.2)] gives the amplitude of the centroid of the propagating FWM pulse. The solid curve represents $[\chi\phi_s(\chi, z = ct = 0)]$, and the dotted curve gives $[\chi\phi_s(\chi, z = ct = 525\ \text{m})]$. The insets shown at the top of the figure display the oscillations inside the Gaussian ω windows at different sampled values of χ evaluated at $z = 525$ m. Note that the amplitudes of these Gaussians are plotted to scale. However, for the sake of illustration, their horizontal dimensions are displayed on a scale that differs from that of the spatial spectrum. The width of the ω Gaussians is $\delta(\omega/c) \cong 8/cT = 1280\ \text{m}^{-1}$, while $\chi_{\max} = 1415\ \text{m}^{-1}$. At low χ values, higher oscillations are introduced into the associated ω windows. The integration over ω in Eq. (3.3) produces negligible contributions from these ω windows centered around such low χ values. This results in a rapid depletion of the corresponding spectral components of the associated spatial sections. From Fig. 3 one can also note that as χ increases the oscillations are noticeably decreased. Hence the higher components of the spatial spectrum hold out for farther distances than the lower ones. Since the area under the $[\chi\phi_s(\chi, z = ct)]$ curve represents the amplitude of the centroid of the pulse as it propagates away from the aperture, then the above analysis explains the behavior of the pulse as it is launched into the $z > 0$ half-space. As the pulse propagates away from its source, the oscillations introduced into the lower ω windows progressively cut off the contributions of the smaller χ spectral components, causing the area under $[\chi\phi_s(\chi, z = ct)]$ to decrease. Consequently, the amplitude of the centroid of the FWM pulse decays as the distance z is increased.

The situation for both the quasi-monochromatic and the broadband signals is quite different from that of the FWM pulse. This can be demonstrated if we study the behavior of the spatial spectrum of those two cases. Substituting Eq. (2.2), with $\omega_0(\chi) = \omega_c$, into Eq. (3.1) gives the spatial spectrum of the quasi-monochromatic signal at any distance z from the aperture, which is explicitly given as

$$\phi_s(\chi, z, t) = \frac{T \exp(-\chi^2 w^2)}{2\pi^{3/2}} \int_0^\infty d\omega \exp[-T^2(\omega - \omega_c)^2] \times \cos\{[\sqrt{(\omega/c)^2 - \chi^2}]z - \omega t\}, \tag{3.4}$$

with $1/T \ll \omega_c$. The parameter controlling the pulse duration T is chosen to have the same value as that of the FWM case. The behavior of the spatial spectrum [Eq. (3.4)] is slightly different from that of the FWM pulse. For the quasi-monochromatic pulse the ω window is centered around a fixed value equal to $4/a_1 \gg 4\sqrt{\beta/a_1}$. The excitation ω window does not sweep the χ spectrum as in the case of the FWM; instead, it supplies the significant temporal spectral components from those surrounding the constant ω_c frequency. This carrier frequency is much larger than the maximum χ components as long as $\beta a_1 \ll 1$. Consequently, the Gaussian ω window can be approximated by the Dirac delta function $\delta(\omega - \omega_c)$. Thus, for all practical purposes, we may consider that the spatial spectrum varies sinusoidally with χ. The frequency of the oscillations introduced over the whole χ spectrum is controlled mainly by z. Figure 4 illustrates this point, where Eq. (3.4) is displayed at various values of z. From the figure it is clear that at $z = 3$ m there are nearly two complete cycles inside the whole spatial spectrum. The two cases of $z = 12$ m and $z = 48$ m clarify the effect of increasing z on the oscillations introduced over the spatial spectrum. The farther the pulse travels, the larger is the number of cycles embodied by the spatial spectrum. Consequently, the integration given in Eq. (3.2), results in a progressively decaying field amplitude as the pulse propagates away from its source.

The effects of the ω window in the integrand of Eq. (3.4) is illustrated in Fig. 5, which is plotted at $z = 6$ m. It can be inferred from the figure that there are hardly any oscillations inside the ω windows, and their amplitude is scaled by the respective values of the cosine term. Hence the depletion of the spectral components does not result

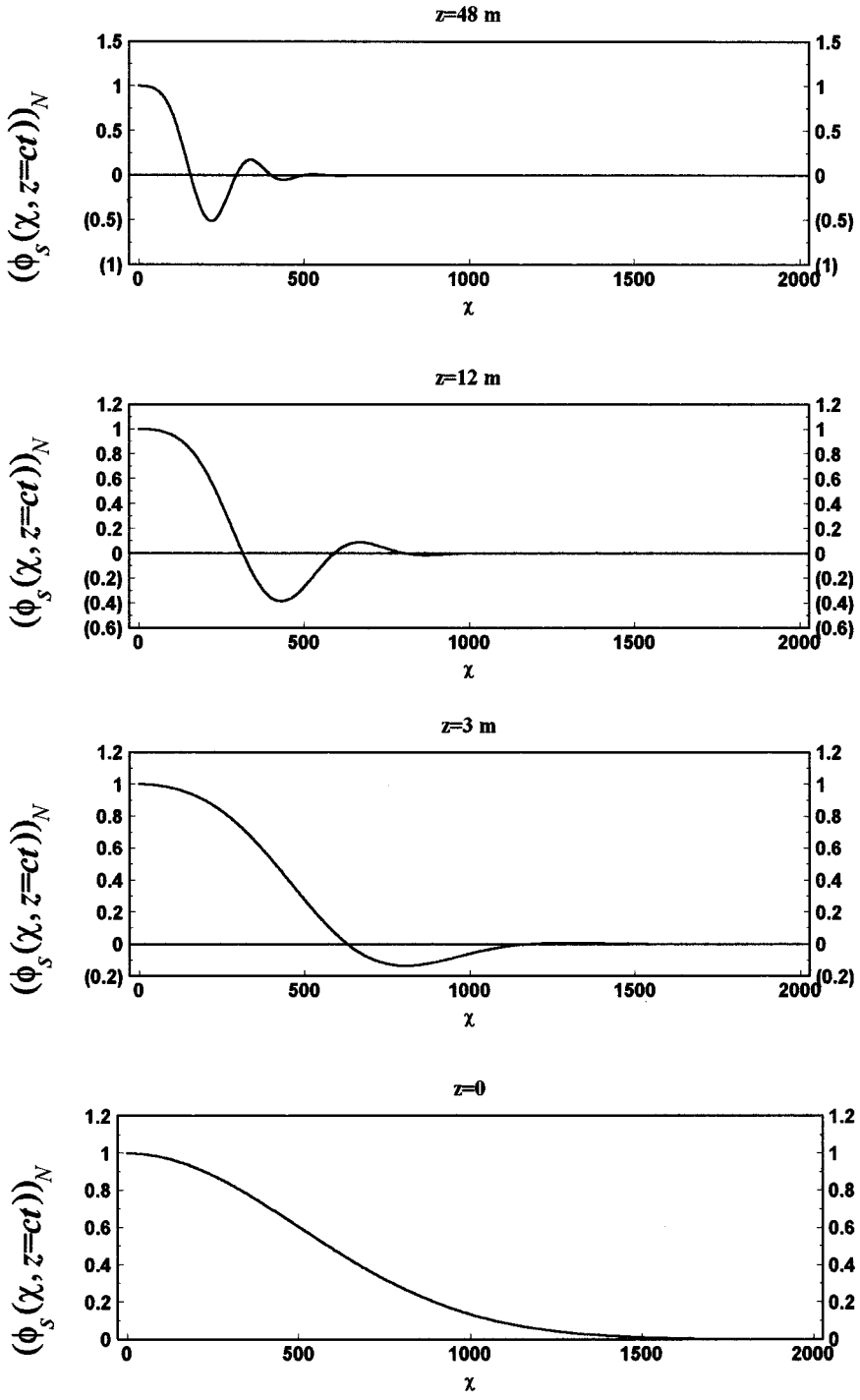

Fig. 6. Depletion of the spatial spectrum of broadband pulse with distance.

from the oscillations incorporated into the ω window. This is the case because the window is centered around a very high frequency and has a relatively narrow bandwidth. The decay of the amplitude of the pulse results mainly from the oscillations introduced over the whole χ spectrum. One should contrast such behavior with the depletion of the spectral content of the FWM pulse that is due to the oscillations introduced into the excitation ω window. In the FWM case the lower spatial spectral components are removed first, while the higher spectral amplitudes are retained with very little changes. In contradistinction, the spatial spectrum of a quasi-monochromatic pulse traveling away from its source experiences progressively increasing oscillations over the whole spectral width. As such, the introduced oscillations result in substantial losses of the net area under the curve representing the spatial spectrum. This in turn causes the amplitude of the quasi-monochromatic pulse to fall off at a fast rate [see Figs. 1(a) and 1(b)].

One should note that in Figs. 1(b), 4, and 5 we have

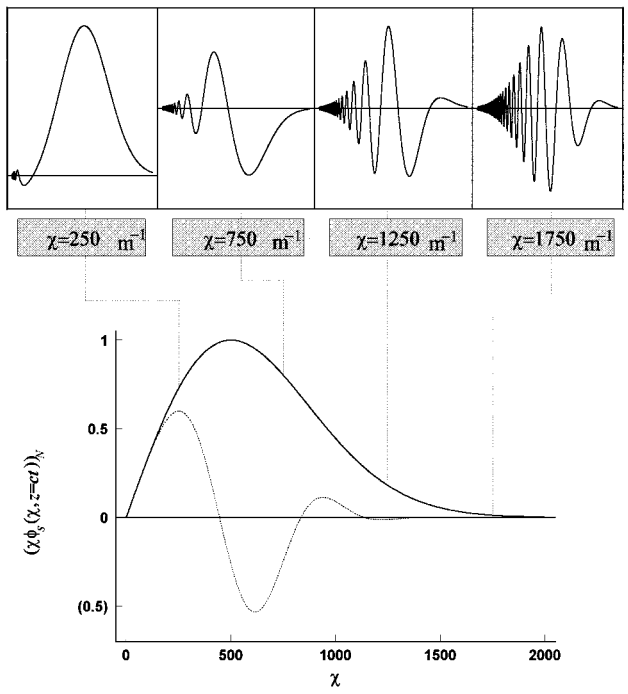

Fig. 7. Oscillations that affect different sections of the spatial spectrum of a broadband pulse at $z = ct = 6$ m. Solid curve, $\chi\phi_s(\chi, z = ct = 0)$; dotted curve, $\chi\phi_s(\chi, z = ct = 6$ m).

limited our discussion to the $z = ct$ point. This point corresponds to the maximum amplitude of the pulse in the near field. In the far-field region the maximum amplitude occurs at a different point. We have confined our analysis, however, to the point $z = ct$ because it suffices to illustrate the introduction of the oscillations over the whole χ spectrum, as in Fig. 4. The maximum amplitude point in the far field would introduce the same oscillations with an extra phase shift. As for Fig. 1(b), the displayed decay of the $z = ct$ point is indistinguishable from the decay of the maximum; we need a logarithmic plot to observe any difference in the amplitudes at these two field points.

Next we consider the effect of increasing the width of the ω window in order to move to the range of broadband signals. The spatial spectrum of such a signal may be obtained by substituting Eqs. (2.2) and (2.3) into Eq. (3.1) to give the same expression as that given in Eq. (3.4) but with $1/T \sim O(\omega_c)$. If we choose $cT = 5 \times 10^{-3}$ mm, the broadband pulse has a longitudinal extension of the same order as a_1, the length of the central portion of the FWM pulse. The spatial spectrum given in Eq. (3.4) is evaluated numerically and is displayed in Fig. 6 at various $z = ct$ points. It seems that the depletion of the spatial spectrum in this case combines some of the features of both the FWM and the quasi-monochromatic signals. The oscillations are introduced over the whole χ spectrum, similarly to the quasi-monochromatic case. The higher components of the spatial spectrum, however, are depleted faster than the lower ones. This is the inverse of the FWM case. Figure 7 displays the oscillations that affect different sections of the spatial spectrum at $z = 6$ m. It is clear that oscillations inside the ω windows are directly proportional to χ. The oscillations introduced at high χ values result in the depletion of those spatial components faster than the ones at lower χ values.

4. EFFECT OF A DERIVATIVE DETECTOR

It is clear from Fig. 3 that the lower-frequency components of the FWM pulse are depleted at a faster rate. Consequently, following the analysis of Ziolkowski and Judkins[13] for detecting time-limited pulses having ultrawide bandwidths, one can design a differentiating receiver that is capable of accessing the higher-frequency portions of the spectrum of the FWM pulse. For practical realization of such derivative antennas, one should refer to the discussion in Ref. 13. Our aim here is to illustrate how such an enhancement in detecting the differentiated signal is achieved. Actually, the result follows systematically from our analysis of the depletion of the spectral content of the FWM pulse. In particular, when the field in Eq. (2.7) is differentiated with respect to t, we obtain

$$\dot{\Psi}(\rho, z, t) = \frac{T}{2\pi^{3/2}} \int_0^\infty d\chi \chi J_0(\chi\rho) \times \int_0^\infty d\omega\omega \exp\{-T^2[\omega - \omega_0(\chi)]^2\} \times \exp(-\chi^2 w^2) \times \sin\{[\sqrt{(\omega/c)^2 - \chi^2}]z - \omega t\}. \quad (4.1)$$

The dot indicates partial differentiation with respect to time. The differentiated signal contains all the ingredients discussed in the preceding sections. Specifically, we have the temporal ω window, the spatial Gaussian waist function, and the oscillatory sinusoidal term. The only difference is having an extra ω factor in the integrand. Such a multiplicative quantity may be perceived as a

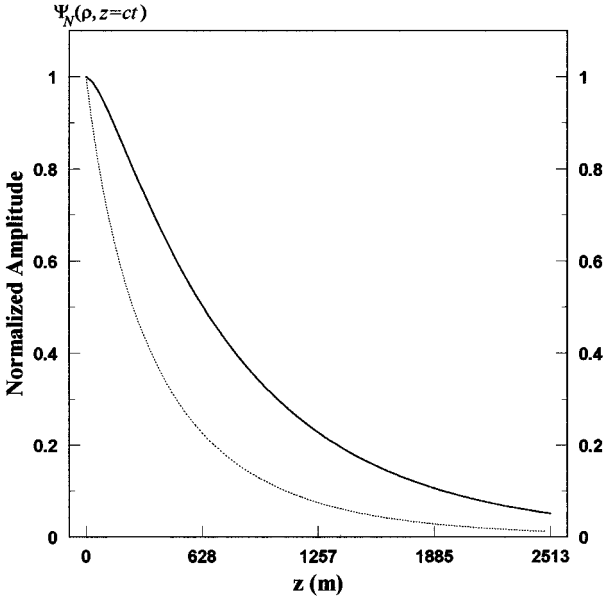

Fig. 8. Effect of a derivative detector on improving the decay pattern of the received FWM signal. Solid curve, amplitude measured by a derivative detector, dotted curve, amplitude detected by a regular receiver.

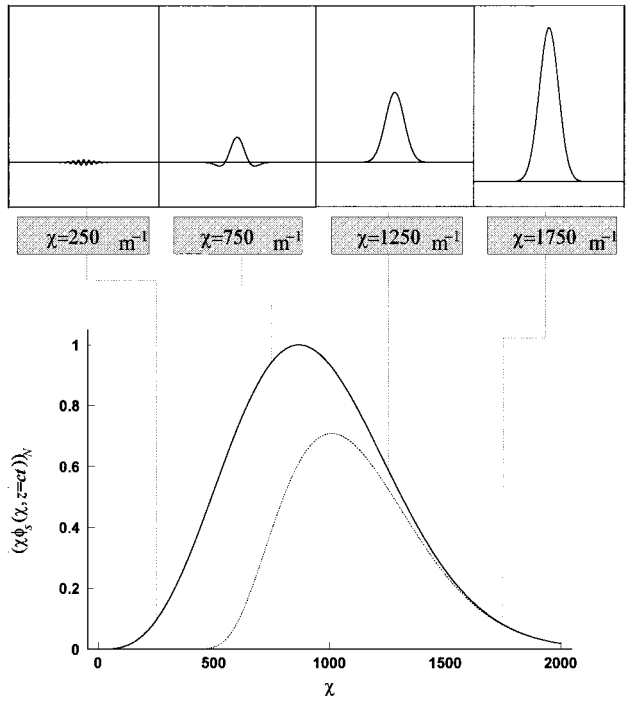

Fig. 9. Effect of a derivative detector on the oscillations that affect different sections of the FWM spatial spectrum at $z = ct = 525.27$ m. Solid curve, $\chi\phi_s(\chi, z = ct = 0)$; dotted curve, $\chi\phi_s(\chi, z = ct = 525.27$ m).

weighting function that emphasizes the contributions of the higher-frequency ω windows; the depletion of the lower spectral components results in a relatively slower decay, as illustrated in Fig. 8. The amplitude of the differentiated centroid of the FWM wave field is normalized relative to that at the aperture. The measured differentiated signal amplitude is plotted as a function of the distance z. The solid curve represents the FWM amplitude measured by a derivative detector, and the dotted curve shows the relative decay of the amplitude detected by a regular receiver. In Fig. 9 we demonstrate how the spatial spectrum corresponding to the differentiated wave field is depleted. The insets show the same oscillations as in Fig. 3; however the higher-frequency ω windows are weighted by a larger ω factor. This leads to a spatial spectrum showing less deterioration than that depicted in Fig. 3. It is important to point out that for wave fields incorporating a carrier frequency, the differentiating receiver makes very little difference even for the broadband case. For the latter excitation the depletion of the spectral components starts with the higher frequencies. Thus not all broadband time-limited signals can benefit from the use of a derivative detector. Only pulses whose low-frequency components are depleted at a faster rate may show the desired enhancement.

5. CONCLUDING REMARKS

In this paper, we have attempted to emphasize the difference between the depletion of the spectral components of the FWM pulse and those of other transient wave fields. It has been shown that dynamic apertures provide an efficient scheme for launching narrow-waisted Gaussian pulses from sources with larger dimensions. A traditional flat, static aperture of the same size fails to send equally narrow pulses to the same extended ranges in the near-to-far-field region. We have demonstrated that the extended ranges of localization of the FWM pulses follow from the spatial–temporal coupling of the pulses spectral components. Such a spectral correlation leads to a radically different process for the depletion of the pulse's spatial spectrum with distance. At the same time, the coupling of the FWM spatial and temporal spectral contents leads to an aperture that varies in size with time. Other excitation procedures may lead to different depletion effects. It is clear from our analysis that the LW pulses generated exhibit slower decay patterns if cT is increased. This yields a narrow ω window spectral distribution. It should be of great interest to extend the ω–χ coupling procedure such that the width of the ω window is reduced without an increase in the size of the aperture or the bandwidth of the generating source.

The study of the depletion of the spectral components of the FWM pulse has revealed the interesting property that the lower-frequency components are removed first. This behavior is not manifested by the quasi-monochromatic and the broadband pulsed wave fields. Consequently, the FWM signal measured by a differentiating receiver exhibits a slower decay rate than the signal received by a regular detector. Such an improvement in the decay rate of the measurement of the differentiated signal can be easily explained by our analysis of the pulse's spectral depletion with distance.

REFERENCES

1. J. N. Brittingham, "Focus wave modes in homogeneous Maxwell's equations: transverse electric mode," J. Appl. Phys. **54**, 1179–1189 (1983).
2. T. T. Wu and R. W. King, "Comments on focus wave modes in homogenous Maxwell's equations: transverse electric mode," J. Appl. Phys. **56**, 2587 (1984).
3. R. W. Ziolkowski, "Exact solutions of the wave equation with complex source locations," J. Math. Phys. **26**, 861–863 (1985).
4. A. M. Shaarawi, I. M. Besieris, and R. W. Ziolkowski, "Localized energy pulse trains launched from an open, semi-infinite, circular waveguide," J. Appl. Phys. **65**, 805–813 (1989).
5. R. W. Ziolkowski, I. M. Besieris, and A. M. Shaarawi, "Localized wave representation of acoustic and electromagnetic radiation," Proc. IEEE **79**, 1371–1378 (1991).
6. R. W. Ziolkowski, "Properties of electromagnetic beams generated by ultra-wide bandwidth pulse-driven arrays," IEEE Trans. Antennas Propag. **40**, 888–905 (1992).
7. A. M. Vengsarkar, I. M. Besieris, A. M. Shaarawi, and R. W. Ziolkowski, "Closed-form, localized wave solutions in optical fiber waveguides," J. Opt. Soc. Am. A **9**, 937–949 (1992).
8. R. W. Ziolkowski, I. M. Besieris, and A. M. Shaarawi, "Aperture realizations of the exact solutions to homogeneous wave-equations," J. Opt. Soc. Am. A **10**, 75–87 (1993).
9. R. Donnelly and R. W. Ziolkowski, "A method of constructing solutions of homogenous partial differential equations: localized waves," Proc. R. Soc. London Ser. A **437**, 673–692 (1992).
10. R. W. Ziolkowski, "Localized transmission of electromagnetic energy," Phys. Rev. A **39**, 2005–2033 (1989).

11. A. M. Shaarawi, R. W. Ziolkowski, and I. M. Besieris, "On the evanescent fields and the causality of the focused wave modes," J. Math. Phys. **36**, 5565–5587 (1995).
12. A. M. Shaarawi, I. M. Besieris, R. W. Ziolkowski, and S. M. Sedky, "Generation of approximate focused-wave-mode pulses from wide-band dynamic Gaussian apertures," J. Opt. Soc. Am. A **12**, 1954–1964 (1995).
13. R. W. Ziolkowski and J. B. Judkins, "Propagation characteristics of ultrawide-bandwidth pulsed Gaussian beams," J. Opt. Soc. Am. A **9**, 2021–2030 (1992).
14. P. M. Morse and H. Feshbach, *Methods of Theoretical Physics* (McGraw-Hill, New York 1953), Sec. 11.3.